Available online at www.sciencedirect.com
SCIENCE DIRECT
Journal of Organometallic Chemistry 691 (2006) 2575–2583
Journal of Organometallic Chemistry
www.elsevier.com/locate/jorganchem

Synthesis, characterization and structural studies of palladium(II) complexes with *N*-(aroyl)-*N*′-(2,4-dimethoxybenzylidene)hydrazines

Sunirban Das, Samudranil Pal *

School of Chemistry, University of Hyderabad, Hyderabad 500 046, India

Received 4 January 2006; received in revised form 26 January 2006; accepted 26 January 2006
Available online 6 March 2006

Abstract

Reactions of $Li_2[PdCl_4]$ with *N*-(aroyl)-*N*′-(2,4-dimethoxybenzylidene)hydrazines (H_2L = (4-R–C_6H_4)C(=O)NHN=CH(2,4-$(CH_3O)_2$-C_6H_3)) in presence of PPh_3 have provided cyclopalladated complexes having the general formula [PdL(PPh_3)] (**1**, **2** and **3** where R = OCH_3, CH_3 and Cl, respectively) and a coordination complex *trans*-[Pd(HL)$(PPh_3)_2$Cl] (**4** where R = NO_2). The complexes have been characterized by elemental analysis, infrared, ^{1}H NMR and electronic absorption spectroscopy. X-ray structures of all the complexes have been determined. In **1**, **2** and **3**, the C,N,O-donor dianionic ligand (L^{2-}) forms two fused five-membered chelate rings at the metal centre. On the other hand, the monoanionic ligand (HL^-) acts as deprotonated amide N-donor in **4**. The strong electron withdrawing effect of the nitro group on the aroyl fragment is possibly responsible for the monodentate amide N-coordinating behavior of HL^- in **4**. The orientation of the 4-methoxy group in **1** is different than that in **2** and **3** due to intramolecular C–H···π interaction in the last two complexes. The structure of **4** shows an apical C–H···Pd interaction involving the azomethine (–CH=N–) group of HL^-. In the crystal lattice of all the structures, various types of intermolecular non-covalent interactions are present. The self-assembly of the molecules of **1**, **2** and **3** leads to two-dimensional networks. The same network observed for **2** and **3** reflects the interchangeability of the chloro and methyl groups due to their similar volumes. In the case of **4**, the complex and the water molecules present in the crystal lattice form parallel homo-chiral helices and finally interhelical interactions lead to a three-dimensional network.

Keywords: Cyclopalladation; Aroylhydrazones; Substituent effect; Crystal structures; Self-assembly

1. Introduction

Thiosemicarbazones and semicarbazones of aromatic aldehydes are known to act as tridentate ligands for Pd(II) and Pt(II) via *ortho*-metallation and can yield cyclometallated complexes having two fused five-membered chelate rings at the metal centre [1–4]. Thiosemicarbazones can coordinate the metal ion as mono- or bianionic C,N,S-donor ligand. On the other hand, semicarbazones are reported to act only as monoanionic C,N,O-donor ligand. No complex containing bianionic C,N,O-donor semicarbazone as ligand is reported so far. In these cyclometallated complexes, the metal–oxygen bond cleaves more easily than the metal–sulfur bond. Aroyl- or acylhydrazones of aromatic aldehydes which are similar to semicarbazones can also act as tridentate C,N,O-donor ligands via cyclometallation at the benzylidene ring [5,6]. Structurally characterized cyclometallated complexes of such ligands are very rare [6]. Recently we have reported the synthesis, reactivities and structures of some cyclopalladated complexes with *N*-(benzoyl)-*N*′-(2,4-dimethoxybenzylidene)hydrazine (H_2L, R = H) which falls in this class of ligands [7]. We have shown that the ligand can behave as mono- as well as bianionic C,N,O-donor. When it is monoanionic (HL^-) the metal–oxygen bond is labile to the nucleophiles. On the other hand, when it is bianionic (L^{2-}) the metal–oxygen bond is inert. The electronic nature of the substituent (R) at the *para* position of the aroyl fragment is

* Corresponding author. Tel.: +91 40 2313 4756; fax: +91 40 2301 2460.
E-mail address: spsc@uohyd.ernet.in (S. Pal).

0022-328X/$ - see front matter © 2006 Elsevier B.V. All rights reserved.
doi:10.1016/j.jorganchem.2006.01.052

expected to affect the acidity of the amide functionality present in H_2L and hence the σ-bonding ability of the coordinating atom (N or O) of the deprotonated amide. If the deprotonated amide functionality binds the metal ion via the N-centre, *ortho*-metallation if any has to occur at the aroyl fragment instead of the benzylidene fragment of the ligand [8,9]. In this work, we have studied the effect of the substituents (R) having different polar effects on the cyclopalladation reactions with *N*-(4-R-benzoyl)-*N*′-(2,4-dimethoxybenzylidene)hydrazines (H_2L). The synthesis, characterization and crystal structures of the complexes isolated in this effort are described in the present account.

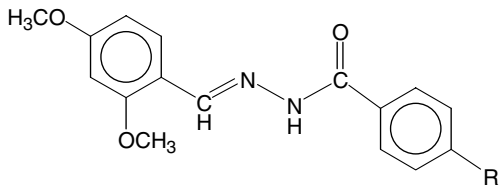

(H_2L, R = OCH_3, CH_3, Cl, NO_2)

2. Experimental

2.1. Materials

The solvents were purified by standard methods [10]. All the chemicals used in this work were of analytical grade available commercially and were used without further purification.

2.2. Physical measurements

Microanalytical (C, H, N) data were obtained with a Thermo Finnigon Flash EZ1112 series elemental analyzer. Room temperature solid state magnetic susceptibilities were measured by using a Sherwood Scientific magnetic susceptibility balance. Solution electrical conductivities were measured with a Digisun DI-909 conductivity meter. IR spectra were collected by using KBr pellets on a Jasco-5300 FT-IR spectrophotometer. A Shimadzu 3101-PC UV/vis/NIR spectrophotometer was used to record the electronic spectra. Proton NMR spectra were recorded on a Bruker 400 MHz spectrometer using $Si(CH_3)_4$ as an internal standard.

2.3. General procedure for the synthesis of Schiff bases

To a methanol solution (20 cm^3) of the appropriate substituted benzoylhydrazine (4.0 mmol) and 2,4-dimethoxybenzaldehyde (4.0 mmol) a few drops of acetic acid were added. The mixture was refluxed for 6 h and then cooled to room temperature. The crystalline solid separated was collected by filtration, washed with cold methanol and finally dried in air.

2.3.1. N-(4-methoxybenzoyl)-N′-(2,4-dimethoxybenzylidene)hydrazine

White solid (86%): M.p. 188–190 °C; Anal. Calc. for $C_{17}H_{18}N_2O_4$: C, 64.96; H, 5.77; N, 8.91. Found: C, 64.9; H, 5.7; N, 8.5%. IR (cm^{-1}): 3167 m (ν_{N-H}), 1636s ($\nu_{C=O}$), 1599s ($\nu_{C=N}$). ^1H NMR (400 MHz) data in $CDCl_3$ (δ (J (Hz))): 3.83, 3.84, 3.86 (3s, 9H, 3 OCH_3); 6.42 (s, 1H, H^3); 6.53 (8) (d, 1H, H^5); 6.94 (8) (d, 2H, H^{11}, H^{13}); 7.83 (8) (d, 2H, H^{10}, H^{14}); 8.07 (8) (d, 1H, H^6); 8.50 (s, 1H, H^7); 9.12 (s, 1H, NH). Electronic spectral data in CH_3CN (λ (nm) (ε (M^{-1} cm^{-1}))): 330 (28200), 297 (18300), 286 (17700), 238 (14800).

2.3.2. N-(4-methylbenzoyl)-N′-(2,4-dimethoxybenzylidene)hydrazine

White solid (86%), M.p. 202–204 °C; Anal. Calc. for $C_{17}H_{18}N_2O_3$: C, 68.44; H, 6.08; N, 9.39. Found: C, 68.4; H, 5.9; N, 9.2%. IR (cm^{-1}): 3202 m (ν_{N-H}), 1639s ($\nu_{C=O}$), 1597s ($\nu_{C=N}$). ^1H NMR (400 MHz) data in $CDCl_3$ (δ (J (Hz))): 2.42 (s, 3H, CH_3), 3.84 (s, 6H, 2 OCH_3), 6.43 (2) (d, 1H, H^3), 6.54 (8) (d, 1H, H^5), 7.26 (7) (d, 2H, H^{11}, H^{13}), 7.75 (7) (d, 2H, H^{10}, H^{14}), 8.09 (8) (d, 1H, H^6), 8.50 (s, 1H, H^7), 9.06 (s, 1H, NH). Electronic spectral data in CH_3CN (λ (nm) (ε (M^{-1} cm^{-1}))): 330 (28100), 297 (16900), 287 (16000), 236 (19300).

2.3.3. N-(4-chlorobenzoyl)-N′-(2,4-dimethoxybenzylidene)hydrazine

White solid (92%): M.p. 180–182 °C. Anal. Calc. for $C_{16}H_{15}N_2O_3Cl$: C, 66.10; H, 5.20; N, 9.64. Found: C, 66.1; H, 5.1; N, 9.3%. IR (cm^{-1}): 3185 m (ν_{N-H}), 1649s ($\nu_{C=O}$), 1597s ($\nu_{C=N}$). ^1H NMR (400 MHz) data in $CDCl_3$ (δ (J (Hz))): 3.83, 3.84 (2s, 6H, 2 OCH_3); 6.42 (s, 1H, H^3); 6.52 (bs, 1H, H^5); 7.43 (8) (d, 2H, H^{11}, H^{13}); 7.80 (8) (d, 2H, H^{10}, H^{14}); 8.04 (bs, 1H, H^6); 8.53 (s, 1H, H^7); 9.21 (s, 1H, NH). Electronic spectral data in CH_3CN (λ (nm) (ε (M^{-1} cm^{-1}))): 330 (26800), 298 (14600), 287 (14000), 236 (20500).

2.3.4. N-(4-nitrobenzoyl)-N′-(2,4-dimethoxybenzylidene)hydrazine

Orange solid (88%): M. p. 222–224 °C. Anal. Calc. for $C_{16}H_{15}N_3O_5$: C, 58.36; H, 4.59; N, 12.76. Found: C, 58.3; H, 4.5; N, 12.4%. IR (cm^{-1}): 3184 m (ν_{N-H}), 1651s ($\nu_{C=O}$), 1599s ($\nu_{C=N}$). ^1H NMR (400 MHz) data in $CDCl_3$ (δ (J (Hz))): 3.85 (s, 6H, 2 OCH_3); 6.44 (s, 1H, H^3); 6.50 (8) (d, 1H, H^5); 7.58 (8) (d, 1H, H^6); 8.10 (8) (d, 2H, H^{10}, H^{14}); 8.31 (8) (d, 2H, H^{11}, H^{13}); 8.57 (s, 1H, H^7); 9.20 (s, 1H, NH). Electronic spectral data in CH_3CN (λ (nm) (ε (M^{-1} cm^{-1}))): 335 (19100), 287sh (18300), 279 (19400), 236 (16100).

2.4. General procedure for the synthesis of complexes (*1*–*4*)

A mixture of $PdCl_2$ (0.5 mmol) and LiCl (1.0 mmol) was taken in 15 cm^3 dry methanol and refluxed with stirring for 1 h. It was then cooled to room temperature and

filtered. The filtrate was added dropwise with stirring to a methanol–acetonitrile (1:2) solution (20 cm^3) of the appropriate Schiff base (H_2L) (0.5 mmol). The mixture was then stirred at room temperature for 3 days followed by another 1 day after addition of an acetonitrile solution (10 cm^3) of PPh_3 (1.0 mmol). The orange solid separated was collected by filtration, washed with methanol and finally dried in air.

2.4.1. [Pd{(4-CH_3O–C_6H_4)C(O)=NN=CH(2,4-(CH_3O)$_2C_6H_2$)}(PPh_3)] (**1**)

Orange solid (70%): Anal. Calc. for $C_{35}H_{31}N_2O_4PPd$: C, 61.73; H, 4.59; N, 4.11. Found: C, 61.6; H, 4.5; N, 4.0%. IR (cm^{-1}): 1576s ($\nu_{C=N}$). ^1H NMR (400 MHz) data in $CDCl_3$ (δ (J (Hz))): 3.03 (s, 3H, OCH_3); 3.72 (s, 3H, OCH_3); 3.82 (s, 3H, OCH_3), 5.41 (s, 1H, H^5); 5.93 (s, 1H, H^3); 6.82 (9) (d, 2H, H^{11}, H^{13}); 7.43–7.73 (m, PPh_3 protons); 7.90 (9) (d, 1H, H^7), 7.91 (9) (d, 2H, H^{10}, H^{14}). Electronic spectral data in CH_3CN (λ (nm) (ε (M^{-1} cm^{-1}))): 489sh (4200), 460 (6500), 438sh (5900), 358 (6500), 343sh (6800), 276sh (25 800), 221 (45 800).

2.4.2. [Pd{(4-CH_3–C_6H_4)C(O)=NN=CH(2,4-(CH_3O)$_2C_6H_2$)}(PPh_3)] (**2**)

Orange solid (77%): Anal. Calc. for $C_{35}H_{31}N_2O_3PPd$: C, 63.21; H, 4.70; N, 4.21. Found: C, 63.1; H, 4.7; N, 3.9%. IR (cm^{-1}): 1562s ($\nu_{C=N}$). ^1H NMR (400 MHz) data in $CDCl_3$ (δ (J (Hz))): 2.35 (s, 3H, CH_3); 3.03 (s, 3H, OCH_3); 3.72 (s, 3H, OCH_3); 5.41 (s, 1H, H^5); 5.93 (s, 1H, H^3); 7.12 (8) (d, 2H, H^{11}, H^{13}); 7.43–7.74 (m, PPh_3 protons); 7.85 (8) (d, 2H, H^{10}, H^{14}); 7.93 (9) (d, 1H, H^7). Electronic spectral data in CH_3CN (λ (nm) (ε (M^{-1} cm^{-1}))): 490sh (3600), 460 (5700), 439sh (5200), 360 (6100), 347sh (6200), 257 (28 500), 221 (43 700).

2.4.3. [Pd{(4-Cl–C_6H_4)C(O)=NN=CH(2,4-(CH_3O)$_2C_6H_2$)}(PPh_3)] (**3**)

Orange solid (75%): Anal. Calc. for $C_{34}H_{28}N_2O_3ClPPd$: C, 59.58; H, 4.12; N, 4.09. Found: C, 59.5; H, 4.1; N, 3.9%. IR (cm^{-1}): 1574s ($\nu_{C=N}$). ^1H NMR (400 MHz) data in $CDCl_3$ (δ (J (Hz))): 3.03 (s, 3H, OCH_3); 3.72 (s, 3H, OCH_3); 5.41 (s, 1H, H^5); 5.93 (s, 1H, H^3); 7.28 (9) (d, 2H, H^{11}, H^{13}); 7.42–7.69 (m, PPh_3 protons), 7.88 (9) (d, 2H, H^{10}, H^{14}); 7.92 (9) (d, 1H, H^7). Electronic spectral data in CH_3CN (λ (nm) (ε (M^{-1} cm^{-1}))): 493sh (4500), 462 (7000), 440sh (6200), 361 (6200), 347sh (6300), 275sh (26 300), 219 (49 400).

2.4.4. trans-[Pd{(4-NO_2–C_6H_4)C(=O)NN=CH(2,4-(CH_3O)$_2C_6H_3$)}(PPh_3)$_2$Cl] (**4**)

Orange solid (77%): Anal. Calc. for $C_{52}H_{44}N_3O_5ClP_2Pd$: C, 62.79; H, 4.46; N, 4.22. Found: C, 62.4; H, 4.4; N, 4.0%. IR (cm^{-1}): 1603s (amide), 1593s ($\nu_{C=N}$). ^1H NMR (400 MHz) data in $CDCl_3$ (δ (J (Hz))): 3.89 (s, 3H, OCH_3); 3.91 (s, 3H, OCH_3); 6.49 (s, 1H, H^3); 6.63 (8) (d, 1H, H^5); 7.06 (8) (d, 1H, H^6); 7.32–7.83 (m, PPh_3 protons); 8.11 (9) (d, 2H, H^{11}, H^{13}); 8.75 (9) (d, 1H, H^{10}); 9.03 (9) (d, 1H, H^{14}); 9.05 (s, 1H, H^7). Electronic spectral data in CH_3CN (λ (nm) (ε (M^{-1} cm^{-1}))): 392 (8500), 355sh (18 100), 315 (32 700), 291sh (30 600), 276sh (28 900), 220 (52 200).

2.5. X-ray crystallography

Single crystals were obtained by slow evaporation of dimethylsulfoxide-acetonitrile (1:2) solutions of the complexes. X-ray data were collected on an Enraf-Nonius Mach-3 single crystal diffractometer using graphite monochromated Mo Kα radiation ($\lambda = 0.71073$ Å) by ω-scan

Table 1
Crystallographic data for **1**, **2**, **3** and **4** · H_2O

Complex	**1**	**2**	**3**	**4** · H_2O
Chemical formula	$PdC_{35}H_{31}N_2O_4P$	$PdC_{35}H_{31}N_2O_3P$	$PdC_{34}H_{28}N_2O_3ClP$	$PdC_{52}H_{46}N_3O_6ClP_2$
Formula weight	680.99	664.99	685.40	1012.71
Crystal system	Triclinic	Triclinic	Triclinic	Orthorhombic
Space group	$P\bar{1}$	$P\bar{1}$	$P\bar{1}$	$P2_12_12_1$
a (Å)	10.020(2)	10.9484(7)	10.8011(11)	15.8207(18)
b (Å)	10.902(2)	10.707(4)	10.8132(18)	15.9343(19)
c (Å)	14.356(3)	13.466(1)	13.507(4)	18.931(2)
α (°)	92.04(3)	95.220(14)	94.52(2)	90.00
β (°)	97.89(3)	100.002(6)	100.873(16)	90.00
γ (°)	90.47(3)	98.391(15)	98.355(10)	90.00
V (Å^3)	1552.4(5)	1526.9(5)	1523.6(6)	4772.5(9)
Z	2	2	2	4
ρ (g cm^{-3})	1.457	1.446	1.494	1.409
μ (mm^{-1})	0.691	0.698	0.787	0.565
Reflections unique	5426	5359	5351	4643
Reflections $I \geqslant 2\sigma_I$	4656	4581	4656	2721
Parameters	391	382	381	594
GOF on F^2	1.132	1.067	1.103	1.191
R_1, wR_2 ($I \geqslant 2\sigma_I$)	0.0395, 0.0949	0.0312, 0.0737	0.0280, 0.0616	0.0640, 0.1537
R_1, wR_2 (all data)	0.0507, 0.1195	0.0417, 0.0779	0.0371, 0.0748	0.1384, 0.1783
Largest peak (e Å^{-3})	0.875	0.520	0.371	0.547

method at 298 K. In each case, unit cell parameters were determined by least-squares fit of 25 reflections having θ values in the range 9–12°. Intensities of 3 check reflections were measured after every 1.5 h during the data collection to monitor the crystal stability. No decay was observed for any of the four crystals. Empirical absorption correction was applied to each dataset based on the ψ-scans [11] of selected reflections. The structures were solved by direct methods and refined on F^2 by full-matrix least-squares procedures. The asymmetric unit of each of **1**, **2**, and **3** contains a single complex molecule while that of **4** contains a complex molecule and a water molecule. For all the structures, non-hydrogen atoms were refined using anisotropic thermal parameters. Hydrogen atoms were included in the structure factor calculation at idealized positions by using a riding model, but not refined. The programs of WINGX [12] were used for data reduction and absorption correction. Structure solution and refinement were performed with the SHELX-97 programs [13]. The ORTEX6a [14] and PLATON [15] packages were used for molecular graphics. Selected crystal and refinement data for **1**, **2**, **3** and **4** · H_2O are listed in Table 1.

3. Results and discussion

3.1. Synthesis and characterization

The Schiff bases *N*-(4-R-benzoyl)-*N*′-(2,4-dimethoxybenzylidene)hydrazines (H_2L, R = OCH_3, CH_3, Cl and NO_2) were obtained in high yields (86–92%) by condensation reactions of 2,4-dimethoxybenzaldehyde and the 4-substituted benzoylhydrazines (1:1 mole ratio) in methanol in presence of catalytic amount of acetic acid. The microanalytical data and the spectroscopic features of all the Schiff bases are consistent with their formulae and structures. In methanol–acetonitrile, the reaction of H_2L with $Li_2[PdCl_4]$ (generated in situ by treatment of one mole equivalent of $PdCl_2$ with two mole equivalents of LiCl) and PPh_3 produces the *ortho*-metallated species having the general formula [PdL(PPh_3)] when R = OCH_3 (**1**), R = CH_3 (**2**) and R = Cl (**3**) in 70–77% yields (Scheme 1). In each of these three complexes (**1**–**3**), the bianionic planar ligand (L^{2-}) acts as tridentate C,N,O-donor and the PPh_3 satisfies the fourth coordination site. However, under the same reaction condition *ortho*-metallation does not occur when R = NO_2 and the complex isolated in 77% yield is *trans*-[Pd(HL)(PPh_3)$_2$Cl] (**4**) where the monoanionic HL^- acts as monodentate deprotonated amide N-donor (Scheme 1). The molecular structures of all the complexes (**1**–**4**) have been confirmed by X-ray crystallography (vide infra). The elemental analysis data are consistent with their molecular formulae found in the X-ray structures. All the four complexes are diamagnetic and electrically non-conducting in solutions.

A plausible explanation for the lack of *ortho*-metallation in the case of nitro substituted Schiff base and the formation of *trans*-[Pd(HL)(PPh_3)$_2$Cl] (**4**) is as follows. The strong electron withdrawing effect of the nitro group at the *para* position with respect to the amide functionality is expected to increase the acidity of the amide proton compared to that in the other three Schiff bases. As a result the corresponding conjugate base will be the weakest. In other words the σ-bonding ability of the coordinating centre of the deprotonated amide functionality will be the lowest or more soft for the nitro substituted ligand than the other ligands. In general, the N-centre is softer than the O-centre in a deprotonated amide group. The Pd(II) being a soft metal ion the difference in softness of the coordinating

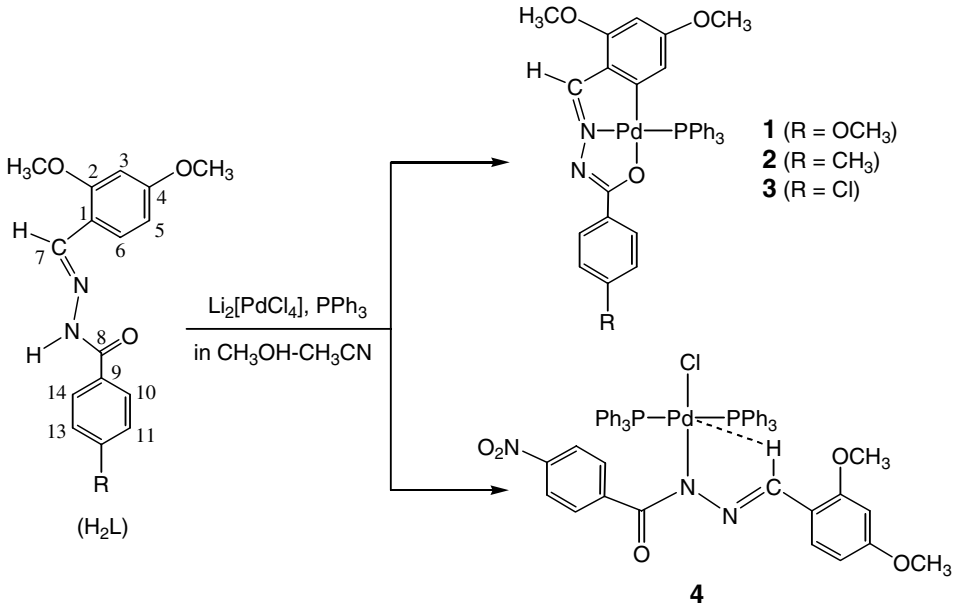

Scheme 1.

atoms can play a major role in coordinating behavior of the ligand. Possibly for this reason amide–N coordination instead of amide–O coordination occurs in **4**. The amide–N coordination does not facilitate the *ortho*-metallation at the benzylidene ring. However, *ortho*-metallation could have taken place at the aroyl fragment ring with the formation of a five-membered ring [8,9]. It is quite likely that the presence of the electron withdrawing nitro group at the *meta* position with respect to the metallation site of the aroyl fragment ring does not help this process also.

3.2. Spectroscopic properties

Infrared spectra of all the compounds have been collected using KBr pellets. The free Schiff bases (H_2L) display the characteristic bands due the N–H and the C=O groups of the amide functionality in the ranges 3167–3202 and 1636–1651 cm^{-1}, respectively [16,17]. The C=N stretch appears as a strong band near 1598 cm^{-1} [1,7]. The spectra of **1**–**3** do not display any band assignable to the N–H or the C=O group of the amide functionality. Thus the amide functionality is in the enolate form and the tridentate ligand (L^{2-}) coordinates the metal centre via the amide–O, the imine–N and the *ortho* C-atom of the benzylidene ring. The X-ray structures confirm this coordination mode of L^{2-} in **1**–**3** (vide infra). The strong band observed in the range 1562–1576 cm^{-1} is assigned to the C=N stretch of the tridentate ligand. The low-energy shift of the C=N stretch as compared to that in the free Schiff bases is consistent with the azomethine N-coordination to the metal ion [7,18]. The X-ray structure shows that there is no *ortho*-metallation and HL^- acts monodentate deprotonated amide–N coordinating ligand in **4** (vide infra). Accordingly the spectrum of **4** does not display any band due to the amide N–H stretch. Two closely spaced strong bands observed at 1603 and 1593 cm^{-1} are attributed to the deprotonated N-coordinating amide [17] and the uncoordinated azomethine (–HC=N–) fragments of HL^-, respectively.

The electronic spectral data for the Schiff bases and the complexes are listed in the experimental section. The spectra of the Schiff bases are very similar and display four intense absorptions in the range 335–236 nm. The spectra of **1**–**3** are also very similar and display seven absorptions in the range 493–219 nm. In contrast the spectrum of **4** is very different and display six absorptions within 392–220 nm. The lower energy additional absorptions for all the complexes are likely to be due to ligand-to-metal charge transfer transitions and the higher energy absorptions are due to ligand based transitions [7].

The ^1H NMR spectra have been recorded using $CDCl_3$ solutions of all the compounds. For the free Schiff bases the protons of the two methoxy groups on the benzylidene fragment appear as two closely spaced singlets when $R = OCH_3$ and Cl and as a singlet when $R = CH_3$ and NO_2 near δ 3.84. The protons of the methoxy and the methyl substituents on the aroyl moiety appear as singlets at δ 3.86 and 2.42, respectively. The N–H proton resonates as a singlet in the range δ 9.06–9.21. The H^3 resonance is observed as a singlet within δ 6.42–6.44. Both H^5 and H^6 resonate as doublets in the ranges δ 6.50–6.54 and 7.58–8.09, respectively. The azomethine proton (H^7) is observed as a singlet within δ 8.50–8.57. Two doublets are observed in the ranges δ 6.94–7.43 and 7.75–7.83 for the Schiff bases with $R = OCH_3$, CH_3 and Cl. The former is attributed to the H^{11} and H^{13} and the latter is assigned to the H^{10} and H^{14} protons. The doublet due to H^{11} and H^{13} shows a clear up-field shift with the progressive increase in the electron releasing ability of the R group. In contrast, for the Schiff base containing the most electron withdrawing NO_2 substituent the doublet due to H^{11} and H^{13} appears at δ 8.31 and that due to H^{10} and H^{14} appears at δ 8.10. The spectrum of none of the complexes shows any signal attributable to the N–H proton. Thus the amide functionality of the ligand is deprotonated in each complex. The absence of the H^6 resonance in the spectra of **1**–**3** and the appearance of H^5 proton as a singlet instead of a doublet at δ 5.41 are consistent with the *ortho*-metallation of the 2,4-dimethoxy benzylidene ring. The significant up-field shift of the H^5 resonance compared to that in the free Schiff bases indicates shielding by the phenyl rings of the PPh_3 which is *cis* to the metallated C-atom (vide infra) [2,6,7]. For the same reason the singlet due to the 4-methoxy group also shows up-field shift. As a result the singlets due to the methoxy groups of the benzylidene ring are relatively well separated (4-OCH_3 at δ 3.03 and 2-OCH_3 at δ 3.72) for **1**–**3** when compared with those for the free Schiff bases. The H^3 proton is observed as a singlet with a small up-field shift (δ 5.93). The azomethine proton (H^7) in **1**–**3** is also up-field shifted (δ 7.90–7.93). This up-field shift is consistent with the weakening of the C=N bond due to the N-coordination and the *trans* disposition of the Pd and the proton around the C=N [7,19–22]. However, unlike the free Schiff bases it appears as a doublet due to the coupling with the ^{31}P nucleus which is *trans* (vide infra) to the N-atom [4,7,21,22]. Two doublets observed in the ranges δ 6.82–7.28 and 7.85–7.91 correspond to the aroyl ring protons. The former is assigned to the H^{11} and H^{13} protons and the latter is assigned to the H^{10} and H^{14} protons. In the spectra of all the complexes (**1**–**4**) the PPh_3 phenyl ring protons appear as multiplets in the range δ 7.32–7.83. Not surprisingly the other features in the spectrum of **4** are different compared to those in the spectra of the *ortho*-metallated species (**1**–**3**). Due to deprotonation of the amide functionality the N–H proton is not observed. The singlets corresponding to the two methoxy groups of the benzylidene ring appear at δ 3.89 and 3.91. The signal at slightly up-field is assigned to the 2-OCH_3 group as it is closer to one of the two PPh_3 ligands (vide infra). The singlet observed at δ 6.49 is assigned to the H^3 proton. The H^5 and H^6 protons appear as two doublets at δ 6.63 and 7.06, respectively. The doublet corresponding to two protons observed at δ 8.11 is assigned to the H^{11} and H^{13} protons. Each of the two doublets observed at δ 8.75 and 9.03 corresponds to single proton. The X-ray structure of **4**

shows that the H^{14} is very close to the uncoordinated imine–N (vide infra). Possibly due to a similar situation in solution the signal due to H^{10} and H^{14} gets separated and appear as two doublets at δ 8.75 and 9.03, respectively. For the free nitro substituted Schiff base the azomethine proton (H^7) resonates as a singlet at δ 8.57. In the spectrum of **4**, a singlet corresponding to a single proton is observed at δ 9.05 The solid state structure of **4** reveals that the azomethine hydrogen of HL^- is very close to the apical coordination site of the metal centre (vide infra). The resonance at δ 9.05 is assigned to the azomethine proton (H^7) considering its down-field appearance [23,24]. A further down-field shift of this signal by about δ 0.1 on cooling to −60 °C supports this assignment and suggests that the C–H···Pd interaction in **4** is possibly more of hydrogen bond type than the agostic bond type [24].

3.3. Description of molecular structures

The molecular structures of **1** and **2** are depicted in Fig. 1. In every respect the structure of **3** (Fig. S1 in supplementary material) is identical with that of **2**. The selected bond parameters associated with the metal ions are listed in Table 2. In each complex, the planar tridentate ligand L^{2-} coordinates the metal ion via the aryl C-atom, the azomethine N-atom and the O-atom of the deprotonated amide functionality forming two fused five-membered rings. The P-atom of PPh_3 occupies the fourth coordination site and completes a CNOP square-planar environment around the Pd(II) centre. The N–N, N–C and C–O bond lengths in the =N–N=C(O^-)– fragment of L^{2-} are consistent with the enolate form of the amide functionality [7,25]. The bond lengths and bond angles associated with the metal ion in **1**–**3** are very similar (Table 2). The Pd–C and Pd–N bond lengths and the C–Pd–N angles are comparable with the values reported for similar *ortho*-palladated complexes with Schiff bases [1–4,6,7,19,20]. The Pd–O bond lengths are comparable to that observed for the analogous complex in which R = H [7]. As expected these are shorter than the Pd–O bond lengths observed for Pd(II) complexes of C,N,O-donor ligands having O-coordinating protonated amide functionality [1,3,6]. The Pd–P [1–4,6,7,19–22] bond lengths are unexceptional. There is a major difference in the molecular conformations of **1**–**3** with respect to the orientation of the methyl group of the 4-methoxy substituent on the benzylidene ring (Fig. 1 and Fig. S1). In **2** and **3**, the methyl group is close to one of the phenyl rings of PPh_3. However, it is away from the same phenyl ring in **1**. It may be noted that the conformation of **1** is identical to that of the analogous complex where R = H [7]. Possibly intramolecular C–H···π interaction [26] involving the methyl C–H and the phenyl ring is primarily responsible for the observed orientation of 4-methoxy methyl group in **2** and **3**. The C15···cg (centroid of the phenyl ring) and H···cg distances are 4.05 and 3.31 Å for **2** and 4.04 and 3.30 Å for **3**. The C15–H···cg angles are 135.5° and 135.1° for **2** and **3**, respectively.

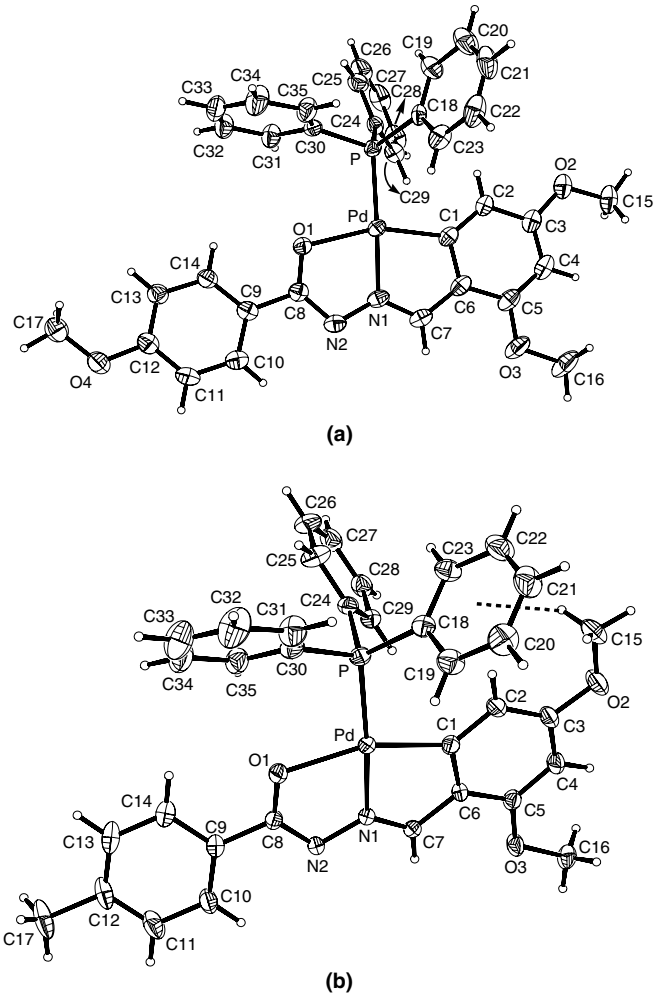

Fig. 1. Molecular structures of [PdL(PPh_3)] (a) **1** (R = OCH_3) and (b) **2** (R = CH_3). All non-hydrogen atoms are represented by their 25% probability thermal ellipsoids.

Table 2
Selected bond lengths (Å) and angles (°) for **1**, **2**, and **3**

Complex	1	2	3
Pd–C(1)	2.006(5)	2.015(3)	2.007(3)
Pd–N(1)	1.983(4)	1.982(2)	1.982(2)
Pd–O(1)	2.107(3)	2.121(2)	2.112(2)
Pd–P	2.2491(12)	2.2638(10)	2.2648(10)
C(1)–Pd–N(1)	82.79(18)	81.58(11)	81.69(11)
C(1)–Pd–O(1)	159.15(16)	158.06(10)	158.08(10)
C(1)–Pd–P	99.62(14)	100.92(9)	100.63(9)
N(1)–Pd–O(1)	76.38(14)	76.56(9)	76.49(9)
N(1)–Pd–P	176.32(11)	174.00(7)	174.63(7)
O(1)–Pd–P	101.23(9)	100.68(6)	100.94(6)

The structure of **4** is shown in Fig. 2. The bond parameters related to the metal ion are listed in Table 3. The Pd(II) centre is in square-planar NP_2Cl coordination geometry assembled by the deprotonated amide–N donor HL^-, the chloride and the two PPh_3 which are *trans* to each other. The Pd–Cl bond length is within the range reported for chloride ligated Pd(II) species [4,7,21,22]. The Pd–N

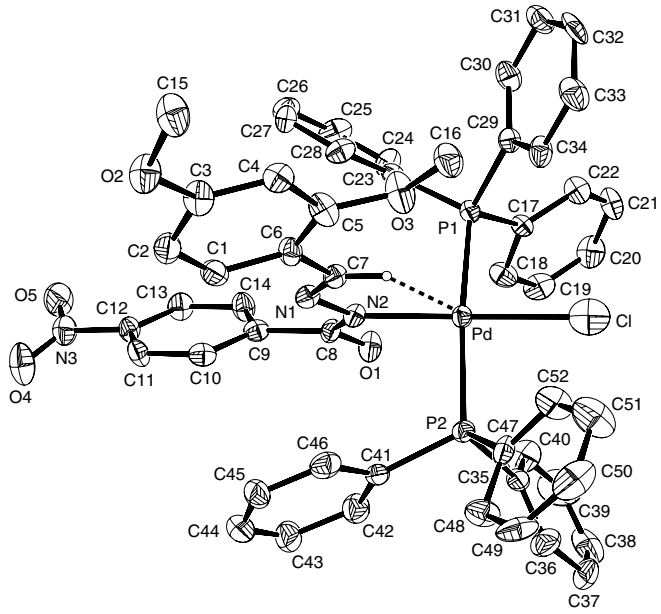

Fig. 2. Molecular structure of $[Pd(HL)(PPh_3)_2Cl]$ (**4**, R = NO_2). All non-hydrogen atoms are represented by their 25% probability thermal ellipsoids. Except the azomethine hydrogen atom all other hydrogen atoms are omitted for clarity.

Table 3
Selected bond lengths (Å) and angles (°) for **4** · H_2O

Pd–Cl	2.391(7)	Pd–N(2)	2.039(11)
Pd–P(1)	2.327(4)	Pd–P(2)	2.322(4)
Cl–Pd–N(2)	178.3(3)	Cl–Pd–P(1)	86.21(19)
Cl–Pd–P(2)	89.1(2)	N(2)–Pd–P(1)	92.7(3)
N(2)–Pd–P(2)	91.8(3)	P(1)–Pd–P(2)	171.98(16)

bond length is longer than the bond lengths reported for deprotonated amide–N coordinated Pd(II) complexes [8,9]. Possibly steric constraints imposed by the two PPh_3 ligands and the monodentate nature of HL^- causes the lengthening of the Pd–N bond in **4**. Two mutually *trans* Pd–P bond lengths in **4** are very similar and as expected they are longer than the Pd–P bond lengths observed in **1**–**3** (Table 2). Interestingly the azomethine (–HC=N–) proton is very close to the metal centre at the apical site (Fig. 2) indicating a C–H···Pd interaction [23,24,27]. The Pd···C7 and Pd···H7 distances and the C7–H7···Pd angle are 3.142(13) and 2.56 Å and 121°, respectively. It may be noted that the plane containing HL^- is roughly orthogonal to the plane containing rest of the molecule of **4** due to the steric constraint forced by the two bulky *trans* oriented PPh_3 ligands (Fig. 2). It is very likely that this steric constraint facilitates the observed C–H···Pd interaction in **4**.

3.4. Intermolecular non-covalent interactions and self-assembly

In the crystal lattice of **1**, one C–H group from each of the three phenyl rings of the ancillary ligand PPh_3 of each molecule are involved in weak intermolecular interactions with three neighboring molecules. The *ortho* C–H and the *meta* C–H of two phenyl rings are close to aroyl ring methoxy O-atoms of two molecules and the *meta* C–H of the third phenyl ring is close to the imine–N of the third molecule. Thus the O-atom of the aroyl ring methoxy group of each molecule is involved in two C–H···O interactions. The C31···O4 and C26···O4 distances are 3.441 and 3.292 Å, respectively. The corresponding C–H···O angles are 150.6 and 148.4°, respectively. The C22···N1 distance and the C22–H···N1 angle are 3.467 Å and 145.5°, respectively. As this sp^2 N-atom is metal coordinated this close contact is most probably due to the C–H···π interaction [26] involving the C=N π-electrons. These C–H···O and C–H···π interactions lead to a two-dimensional layered structure of **1** in the solid state (Fig. 3). In all likelihood the C–H···O interactions are primarily responsible for the two-dimensional network of the molecules which is further supported by the C–H···π interactions.

It is known that the crystal structures of chloro and methyl group containing molecules which are otherwise identical do not change due to the similar sizes of these two groups [28]. The molecules of **2** and **3** provide examples of such species. Indeed the crystal packing of **2** (Fig. 4) and **3** (Fig. S2 in supplementary material) are found to be essentially identical. In both cases, the metal uncoordinated N-atom (N2) of the deprotonated amide functionality participates in C–H···N interaction with the *para* C–H (C27–H27 for **2** and C26–H26 for **3**) of one of the phenyl rings of PPh_3 belonging to a neighboring molecule. The C···N distances and the C-H···N angles are 3.295 Å and 150.2° for **2** and 3.296 Å and 146.9° for **3**. These intermolecular C–H···N interactions lead to a one-dimensional ordering of the molecules in each case. The same phenyl ring that is involved in the C–H···N interaction is also close to the methyl (for **2**) or chloro (for **3**) substituent on the aroyl group of another neighboring molecule. The C17···C28 distance and C12–C17···C28 angle are 3.329 Å and 177.4°, respectively, for **2**, while the Cl···C27 distance and C12-Cl···C27 angle are 3.197 Å and 171.6°, respectively, for **3**. These geometrical parameters indicate that

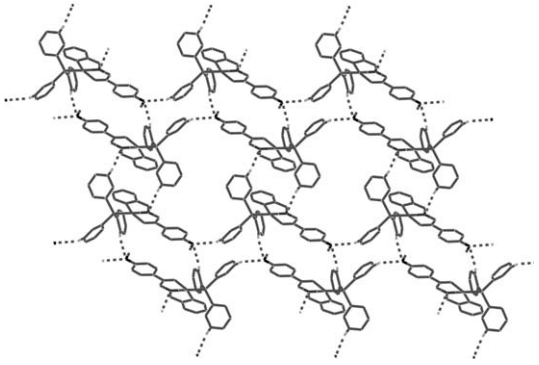

Fig. 3. Two-dimensional network of **1** in the crystal lattice. The methoxy groups on the 2,4-dimethoxybenzylidene fragment and all the hydrogen atoms except those of the three phenyl ring C–H groups involved in intermolecular interactions are omitted for clarity.

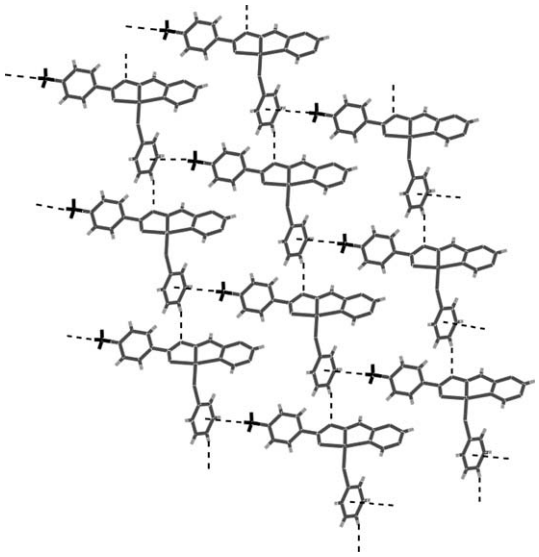

Fig. 4. Two-dimensional network of **2** in the crystal lattice. Two phenyl rings of the PPh_3 and the methoxy groups of the 2,4-dimethoxybenzylidene fragment are omitted for clarity.

C–H···π interaction [26] in **2** and C–Cl···π interaction [29,30] in **3** cannot be ruled out. As these C–H···π and C–Cl···π interactions are roughly orthogonal to the C–H···N interactions, a two-dimensional layered structure is formed in both cases (Fig. 4 and Fig. S2).

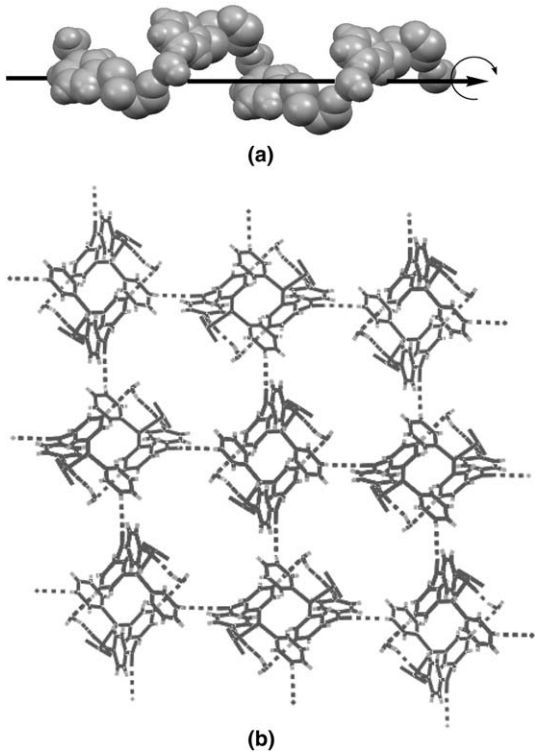

Fig. 5. (a) The helical packing of $\mathbf{4}\cdot H_2O$ along the *a*-axis. For a better view only the (=N–N(PdPPh)–C(=O)–)·H_2O fragment is shown. (b) The projection of the three-dimensional network of $\mathbf{4}\cdot H_2O$ onto the *bc*-plane. For clarity 2,4-dimethoxybenzylidene fragment, one PPh_3 and one phenyl ring of the second PPh_3 are not shown.

In the crystal lattice of $\mathbf{4}\cdot H_2O$, the water molecule and the O-atom (O1) of the N-coordinated amide functionality of HL^- are involved in a reasonably strong O–H···O hydrogen bond. The O6···O1 distance and the O6–H···O1 angle are 2.736 Å and 156.3°, respectively. In addition to this, the water O-atom also acts as acceptor in a weak C–H···O interaction where the C–H group belongs to one of the phenyl rings of PPh_3. The O6···C31 distance and the C31–H···O6 angle are 3.424 Å and 167.9°, respectively. These O–H···O and C–H···O interactions lead to a left-handed helical structure that propagates along the crystallographic *a*-axis (Fig. 5). The parallel homo-chiral helices are connected by a second C–H···O interaction which involves a PPh_3 phenyl ring C–H group and one of the O-atoms of the nitro substituent on the aroyl fragment of HL^-. The O4···C19 distance and the C19–H···O4 angle are 3.259 Å and 130.3°, respectively. Due to these interhelical C–H···O interactions a three-dimensional network of $\mathbf{4}\cdot H_2O$ is formed in the crystal lattice (Fig. 5).

4. Conclusion

The synthesis, properties and X-ray structures of four new square-planar Pd(II) complexes with the Schiff bases *N*-(4-R-benzoyl)-*N*′-(2,4-dimethoxybenzylidene)hydrazines (H_2L) are described. The Schiff bases differ by the substituent (R = OCH_3, CH_3, Cl and NO_2) present in the aroyl fragment. Cyclopalladated species of general formula [PdL(PPh_3)] are isolated when R = OCH_3, CH_3 and Cl. On the other hand, for R = NO_2 the coordination complex *trans*-[Pd(HL)(PPh_3)$_2$Cl] is obtained. In [PdL(PPh_3)], L^{2-} acts as a tridentate C,N,O-donor ligand, while HL^- in *trans*-[Pd(HL)(PPh_3)$_2$Cl] is a monodentate deprotonated amide–N donor ligand. The structure of *trans*-[Pd(HL)(PPh_3)$_2$Cl] reveals that the azomethine (–CH=N–) hydrogen is very close to the apical site of the metal centre suggesting a C–H···Pd interaction. The solution proton NMR data also indicate the presence and predominantly hydrogen bond character of this C–H···Pd interaction. The self-assembly of all the three cyclopalladated complexes via intermolecular non-covalent interactions such as C–H···N, C–H···O, C–H···π and C–Cl···π generates two-dimensional layered structures. The crystal packing patterns of the two complexes where R = CH_3 and Cl are identical but different than that of the complex where R = OCH_3. This observation is in accordance with the chloro-methyl exchange rule. The hydrated molecules of *trans*-[Pd(HL)(PPh_3)$_2$Cl] form a helical structure via O–H···O and C–H···O interactions and finally inter-helical C–H···O interactions lead to a three-dimensional network.

Acknowledgements

Financial support for this work was provided by the Council of Scientific and Industrial Research (CSIR), New Delhi (Grant No. 01(1880)/03/EMR-II). X-ray crystallographic studies were performed at the National Single

Crystal Diffractometer Facility, School of Chemistry, University of Hyderabad (funded by the Department of Science and Technology, New Delhi). We thank the University Grants Commission, New Delhi for the facilities provided under the UPE and CAS programs. Mr. S. Das thanks the CSIR, New Delhi for a research fellowship.

Appendix A. Supplementary data

Figures depicting the molecular structure of **3** (Fig. S1) and the two-dimensional network of **3** (Fig. S2). Crystallographic data have been deposited with the Cambridge Crystallographic Data Centre (deposition numbers are CCDC-294177, CCDC-294178, CCDC-294179 and CCDC-294180 for **1**, **2**, **3** and **4** · H_2O, respectively). Copies of this information can be obtained free of charge from The Director, CCDC, 12, Union Road, Cambridge CB2 1EZ, UK (fax: +44 1223 336033; e-mail: deposit@ccdc.cam.ac.uk or http://www.ccdc.cam.ac.uk). Supplementary data associated with this article can be found, in the online version, at doi:10.1016/j.jorganchem.2006.01.052.

References

[1] J.M. Vila, T. Pereira, J.M. Ortigueira, M. López-Torres, A. Castiñeiras, D. Lata, J.J. Fernández, A. Fernández, J. Organomet. Chem. 556 (1998) 21.
[2] J.M. Vila, M.T. Pereira, J.M. Ortigueira, M. Graña, D. Lata, A. Suárez, J.J. Fernández, A. Fernández, M. López-Torres, H. Adams, J. Chem. Soc., Dalton Trans. (1999) 4193.
[3] A. Fernández, M. López-Torres, A. Suárez, J.M. Ortigueira, T. Pereira, J.J. Fernández, J.M. Vila, H. Adams, J. Organomet. Chem. 598 (2000) 1.
[4] A. Amoedo, M. Graña, J. Martínez, T. Pereira, M. López-Torres, A. Fernández, J.J. Fernández, J.M. Vila, Eur. J. Inorg. Chem. (2002) 613.
[5] M. Nonoyama, M. Sugimoto, Inorg. Chim. Acta 35 (1979) 131.
[6] S. Tollari, G. Palmisano, F. Dematrin, M. Grassi, S. Magnaghi, S. Cenini, J. Organomet. Chem. 488 (1995) 79.
[7] S. Das, S. Pal, J. Organomet. Chem. 689 (2004) 352.
[8] G.J. Palenik, T.J. Giordano, J. Chem. Soc., Dalton Trans. (1987) 1175.
[9] A. Bacchi, M. Carcelli, M. Costa, P. Pelagatti, C. Pelizzi, G. Pelizzi, J. Chem. Soc., Dalton Trans. (1996) 4239.
[10] D.D. Perrin, W.L.F. Armarego, D.P. Perrin, Purification of Laboratory Chemicals, second ed., Pergamon, Oxford, 1983.
[11] A.C.T. North, D.C. Philips, F.S. Mathews, Acta Crystallogr., Sect. A 24 (1968) 351.
[12] L.J. Farrugia, J. Appl. Crystallogr. 32 (1999) 837.
[13] G.M. Sheldrick, SHELX-97, University of Göttingen, Göttingen, Germany, 1997.
[14] P. McArdle, J. Appl. Crystallogr. 28 (1995) 65.
[15] A.L. Spek, PLATON A Multipurpose Crystallographic Tool, Utrecht University, Utrecht, The Netherlands, 2002.
[16] R.M. Siverstein, F.X. Webster, Spectrometric Identification of Organic Compounds, sixth ed., Wiley, New York, 1998, p. 101.
[17] K. Nakamoto, Infrared and Raman Spectra of Inorganic and Coordination Compounds, fourth ed., Wiley, New York, 1986, pp. 242–244.
[18] S.N. Pal, S. Pal, Polyhedron 22 (2003) 867.
[19] J. Albert, A. González, J. Granell, R. Moragas, C. Puerta, P. Valegra, Organometallics 16 (1997) 3775.
[20] X. Riera, A. Caubet, C. López, V. Moreno, X. Solans, M. Fontbardía, Organometallics 19 (2000) 1384.
[21] C. Cativiela, L.R. Falvello, J.C. Ginés, R. Navaro, E.P. Urriolabeitia, New J. Chem. 25 (2001) 344.
[22] J. Albert, M. Gómez, J. Granell, J. Sales, Organometallics 9 (1990) 1405.
[23] D.M. Roe, P.M. Bailey, K. Moseley, P.M. Maitles, J. Chem. Soc., Chem. Commun. 1273 (1972).
[24] W. Yao, O. Eisenstein, R.H. Crabtree, Inorg. Chim. Acta 254 (1997) 105.
[25] R. Raveendran, S. Pal, Polyhedron 24 (2005) 57.
[26] M. Nishio, Cryst. Eng. Commun. 6 (2004) 130.
[27] G. Minghetti, M.A. Cinellu, A.L. Bandini, G. Banditelli, F. Demartin, M. Manassero, J. Organomet. Chem. 315 (1986) 387.
[28] G.R. Desiraju, J.A.R.P. Sarma, Proc. Indian Acad. Sci. (Chem. Sci.) 96 (1986) 599.
[29] M.D. Prasanna, T.N. Guru Row, Cryst. Eng. 3 (2000) 135.
[30] H. Adams, S.L. Cockroft, C. Guardigli, C.A. Hunter, K.R. Lawson, J. Perkins, S.E. Spey, C.J. Urch, R. Ford, Chem. BioChem. 5 (2004) 657.